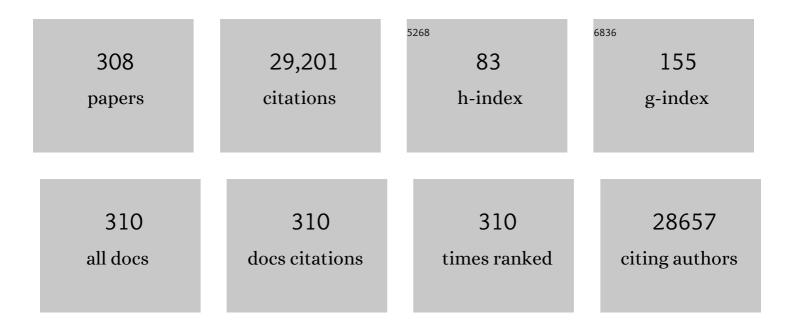
## Nam Hoon Kim

List of Publications by Year in descending order

Source: https://exaly.com/author-pdf/58748/publications.pdf Version: 2024-02-01



#	Article	IF	CITATIONS
1	Ni-nanoclusters hybridized 1T–Mn–VTe2 mesoporous nanosheets for ultra-low potential water splitting. Applied Catalysis B: Environmental, 2022, 301, 120780.	20.2	32
2	Dual-functional Co5.47N/Fe3N heterostructure interconnected 3D N-doped carbon nanotube-graphene hybrids for accelerating polysulfide conversion in Li-S batteries. Chemical Engineering Journal, 2022, 427, 131774.	12.7	38
3	Mo and Zn-Dual doped CuxO nanocrystals confined High-Conductive Cu arrays as novel sensitive sensor for neurotransmitter detection. Journal of Colloid and Interface Science, 2022, 606, 1031-1041.	9.4	2
4	Rational manipulation of 3D hierarchical oxygenated nickel tungsten selenide nanosheet as the efficient bifunctional electrocatalyst for overall water splitting. Chemical Engineering Journal, 2022, 430, 132888.	12.7	29
5	Rapid effective reduction by microwave-irradiated thermal reaction for large-scale production of high-quality reduced graphene oxide. Carbon, 2022, 187, 330-337.	10.3	15
6	A Flexible and Transparent Zincâ€Nanofiber Network Electrode for Wearable Electrochromic, Rechargeable Znâ€Ion Battery. Small, 2022, 18, e2104462.	10.0	50
7	Recent engineering advances in nanocatalysts for NH3-to-H2 conversion technologies. Nano Energy, 2022, 94, 106929.	16.0	15
8	Efficient synergism of NiO-NiSe2 nanosheet-based heterostructures shelled titanium nitride array for robust overall water splitting. Journal of Colloid and Interface Science, 2022, 612, 121-131.	9.4	10
9	Advanced interfacial engineering of oxygen-enriched Fe Sn1â^'OSe nanostructures for efficient overall water splitting and flexible zinc-air batteries. Applied Catalysis B: Environmental, 2022, 305, 120924.	20.2	33
10	Transition metal nanoparticles as electrocatalysts for ORR, OER, and HER. , 2022, , 49-83.		0
11	Fabrication of impermeable dense architecture containing covalently stitched graphene oxide/boron nitride hybrid nanofiller reinforced semi-interpenetrating network for hydrogen gas barrier applications. Journal of Materials Chemistry A, 2022, 10, 4376-4391.	10.3	15
12	Uniformly Controlled Treble Boundary Using Enriched Adsorption Sites and Accelerated Catalyst Cathode for Robust Lithium–Sulfur Batteries. Advanced Energy Materials, 2022, 12, .	19.5	87
13	A 3D hierarchical network derived from 2D Fe-doped NiSe nanosheets/carbon nanotubes with enhanced OER performance for overall water splitting. Journal of Materials Chemistry A, 2022, 10, 3102-3111.	10.3	48
14	Modulating heterointerfaces of tungsten incorporated CoSe/Co <sub>3</sub> O <sub>4</sub> as a highly efficient electrocatalyst for overall water splitting. Journal of Materials Chemistry A, 2022, 10, 3782-3792.	10.3	35
15	Ni Single Atoms and Ni Phosphate Clusters Synergistically Triggered Surfaceâ€Functionalized MoS <sub>2</sub> Nanosheets for Highâ€performance Freshwater and Seawater Electrolysis. Energy and Environmental Materials, 2022, 5, 1340-1349.	12.8	20
16	Bifunctional P-Intercalated and Doped Metallic (1T)-Copper Molybdenum Sulfide Ultrathin 2D-Nanosheets with Enlarged Interlayers for Efficient Overall Water Splitting. ACS Applied Materials & Interfaces, 2022, 14, 14492-14503.	8.0	39
17	Freestanding Binder-Free Electrodes with Nanodisk-Needle-like MnCuCo-LTH and Mn <sub>1</sub> Fe <sub>2</sub> S <sub>2</sub> Porous Microthorns for High-Performance Quasi-Solid-State Supercapacitors. ACS Applied Materials & Interfaces, 2022, 14, 12523-12537.	8.0	10
18	Co-MOF@MXene-carbon nanofiber-based freestanding electrodes for a flexible and wearable quasi-solid-state supercapacitor. Chemical Engineering Journal, 2022, 437, 135338.	12.7	58

#	Article	IF	CITATIONS
19	Single (Ni, Fe) atoms and ultrasmall Core@shell Ni@Fe nanostructures Dual-implanted CNTs-Graphene nanonetworks for robust Zn- and Al-Air batteries. Chemical Engineering Journal, 2022, 440, 135781.	12.7	24
20	Interface engineering induced electrocatalytic behavior in core-shelled CNTs@NiP2/NbP heterostructure for highly efficient overall water splitting. Chemical Engineering Journal, 2022, 442, 136120.	12.7	35
21	Rh single atoms/clusters confined in metal sulfide/oxide nanotubes as advanced multifunctional catalysts for green and energy-saving hydrogen productions. Applied Catalysis B: Environmental, 2022, 313, 121430.	20.2	30
22	Cation and anion (de)intercalation into MXene/Perovskite oxides for high-rate intercalation pseudocapacitance. Energy Storage Materials, 2022, 50, 86-95.	18.0	28
23	Atomic Heterointerface Engineering of Ni <sub>2</sub> Pâ€NiSe <sub>2</sub> Nanosheets Coupled ZnPâ€Based Arrays for Highâ€Efficiency Solarâ€Assisted Water Splitting. Advanced Functional Materials, 2022, 32, .	14.9	49
24	Hybridized bimetallic phosphides of Ni–Mo, Co–Mo, and Co–Ni in a single ultrathin-3D-nanosheets for efficient HER and OER in alkaline media. Composites Part B: Engineering, 2022, 239, 109992.	12.0	96
25	Fibrous asymmetric supercapacitor based on wet spun MXene/PAN Fiber-derived multichannel porous MXene/CF negatrode and NiCo2S4 electrodeposited MXene/CF positrode. Chemical Engineering Journal, 2022, 449, 137732.	12.7	44
26	A hybrid trimetallic–organic framework-derived N, C co-doped Ni–Fe–Mn–P ultrathin nanosheet electrocatalyst for proficient overall water-splitting. Journal of Materials Chemistry A, 2022, 10, 16457-16467.	10.3	41
27	Multi-interfacial engineering of IrOx clusters coupled porous zinc Phosphide-Zinc phosphate heterostructure for efficient water splitting. Applied Surface Science, 2022, 600, 154206.	6.1	8
28	Single platinum atoms implanted 2D lateral anion-intercalated metal hydroxides of Ni2(OH)2(NO3)2 as efficient catalyst for high-yield water splitting. Applied Catalysis B: Environmental, 2022, 317, 121684.	20.2	18
29	Recent progress on single atom/sub-nano electrocatalysts for energy applications. Progress in Materials Science, 2021, 115, 100711.	32.8	27
30	0D to 3D carbon-based networks combined with pseudocapacitive electrode material for high energy density supercapacitor: A review. Chemical Engineering Journal, 2021, 403, 126352.	12.7	755
31	Worm-like gold nanowires assembled carbon nanofibers-CVD graphene hybrid as sensitive and selective sensor for nitrite detection. Journal of Colloid and Interface Science, 2021, 583, 425-434.	9.4	36
32	Recent advances in MXene-based nanocomposites for electrochemical energy storage applications. Progress in Materials Science, 2021, 117, 100733.	32.8	97
33	Core cation tuned MxCo3-xS4@NiMoS4 [MÂ=ÂNi, Mn, zn] core–shell nanomaterials as advanced all solid-state asymmetric supercapacitor electrodes. Chemical Engineering Journal, 2021, 405, 127046.	12.7	39
34	Fabrication of hierarchical Zn–Ni–Co–S nanowire arrays and graphitic carbon nitride/graphene for solid-state asymmetric supercapacitors. Applied Surface Science, 2021, 542, 148564.	6.1	35
35	Pragmatically designed tetragonal copper ferrite super-architectures as advanced multifunctional electrodes for solid-state supercapacitors and overall water splitting. Chemical Engineering Journal, 2021, 415, 127779.	12.7	16
36	Nanostructured CeO2/NiV–LDH composite for energy storage in asymmetric supercapacitor and as methanol oxidation electrocatalyst. Chemical Engineering Journal, 2021, 417, 128019.	12.7	72

#	Article	IF	CITATIONS
37	Two-dimensional materials modified layered double hydroxides: A series of fillers for improving gas barrier and permselectivity of poly(vinyl alcohol). Composites Part B: Engineering, 2021, 207, 108568.	12.0	32
38	Rational Engineering Co <sub>x</sub> O <sub>y</sub> Nanosheets via Phosphorous and Sulfur Dual oupling for Enhancing Water Splitting and Zn–Air Battery. Advanced Functional Materials, 2021, 31, 2007822.	14.9	44
39	All-solid-state asymmetric supercapacitor with MWCNT-based hollow NiCo2O4 positive electrode and porous Cu2WS4 negative electrode. Chemical Engineering Journal, 2021, 415, 128188.	12.7	27
40	Development of hierarchically structured nanosheet arrays of CuMnO2-MnxOy@graphene foam as a nanohybrid electrode material for high-performance asymmetric supercapacitor. Journal of Alloys and Compounds, 2021, 858, 158343.	5.5	21
41	Polymer nanocomposites for energy-related applications. , 2021, , 215-248.		Ο
42	Novel cobalt-doped molybdenum oxynitride quantum dot@N-doped carbon nanosheets with abundant oxygen vacancies for long-life rechargeable zinc–air batteries. Journal of Materials Chemistry A, 2021, 9, 9092-9104.	10.3	41
43	Metal organic framework-derived cobalt telluride-carbon porous structured composites for high-performance supercapacitor. Composites Part B: Engineering, 2021, 211, 108624.	12.0	45
44	Hierarchical Co and Nb dual-doped MoS2 nanosheets shelled micro-TiO2 hollow spheres as effective multifunctional electrocatalysts for HER, OER, and ORR. Nano Energy, 2021, 82, 105750.	16.0	220
45	Strongly stabilized integrated bimetallic oxide of Fe2O3-MoO3 Nano-crystal entrapped N-doped graphene as a superior oxygen reduction reaction electrocatalyst. Chemical Engineering Journal, 2021, 410, 128358.	12.7	47
46	Singleâ€Atom Coâ€Decorated MoS <sub>2</sub> Nanosheets Assembled on Metal Nitride Nanorod Arrays as an Efficient Bifunctional Electrocatalyst for pHâ€Universal Water Splitting. Advanced Functional Materials, 2021, 31, 2100233.	14.9	108
47	Fe and P Doped 1T-Phase Enriched WS23D-Dendritic Nanostructures for Efficient Overall Water Splitting. Applied Catalysis B: Environmental, 2021, 286, 119897.	20.2	88
48	3D nickel molybdenum oxyselenide (Ni1-xMoxOSe) nanoarchitectures as advanced multifunctional catalyst for Zn-air batteries and water splitting. Applied Catalysis B: Environmental, 2021, 286, 119909.	20.2	72
49	Alkaline Water Splitting Enhancement by MOFâ€Derived Fe–Co–Oxide/Co@NCâ€mNS Heterostructure: Boosting OER and HER through Defect Engineering and In Situ Oxidation. Small, 2021, 17, e2101312.	10.0	166
50	Dual-coupling ultrasmall iron-Ni2P into P-doped porous carbon sheets assembled CuxS nanobrush arrays for overall water splitting. Nano Energy, 2021, 84, 105861.	16.0	62
51	Novel core-shell CuMo-oxynitride@N-doped graphene nanohybrid as multifunctional catalysts for rechargeable zinc-air batteries and water splitting. Nano Energy, 2021, 85, 105987.	16.0	89
52	Bifunctional Catalyst Derived from Sulfur-Doped VMoO <sub><i>x</i> </sub> Nanolayer Shelled Co Nanosheets for Efficient Water Splitting. ACS Applied Materials & Interfaces, 2021, 13, 42944-42956.	8.0	26
53	Cobalt-doped cerium oxide nanocrystals shelled 1D SnO2 structures for highly sensitive and selective xanthine detection in biofluids. Journal of Colloid and Interface Science, 2021, 600, 299-309.	9.4	11
54	Ruthenium single atoms implanted continuous MoS2-Mo2C heterostructure for high-performance and stable water splitting. Nano Energy, 2021, 88, 106277.	16.0	68

#	Article	IF	CITATIONS
55	Copper-Incorporated heterostructures of amorphous NiSex/Crystalline NiSe2 as an efficient electrocatalyst for overall water splitting. Chemical Engineering Journal, 2021, 422, 130048.	12.7	54
56	Activated CuNi@Ni Core@shell structures via oxygen and nitrogen dual coordination assembled on 3D CNTs-graphene hybrid for high-performance water splitting. Applied Catalysis B: Environmental, 2021, 294, 120263.	20.2	44
57	Covalently bonded boron nitride quantum dot and reduced graphene oxide composite electrode for highly efficient supercapacitors. Composites Part B: Engineering, 2021, 222, 109089.	12.0	21
58	Rational construction of Au@Co2N0.67 nanodots-interspersed 3D interconnected N-graphene hollow sphere network for efficient water splitting and Zn-air battery. Nano Energy, 2021, 89, 106420.	16.0	26
59	Preparation of functionalized MXene-stitched-graphene oxide/poly (ethylene-co-acrylic acid) nanocomposite with enhanced hydrogen gas barrier properties. Journal of Membrane Science, 2021, 640, 119839.	8.2	29
60	Highly Effective Freshwater and Seawater Electrolysis Enabled by Atomic Rhâ€Modulated Co oO Lateral Heterostructures. Small, 2021, 17, e2103826.	10.0	47
61	Efficient energy storage performance of in situ grown Co3V2O8-RGO composite nanostructure for high performance asymmetric Co3V2O8-RGO//RGO supercapacitors and consequence of magnetic field induced enhanced capacity. Composites Part B: Engineering, 2021, 227, 109384.	12.0	17
62	Interfacial engineering for design of novel 2D cobalt sulfide-Mxene heterostructured catalyst toward alkaline water splitting. Functional Composites and Structures, 2021, 3, 045005.	3.4	18
63	Hierarchical 3D structured nanoporous Co <sub>9</sub> S <sub>8</sub> @Ni <sub><i>x</i></sub> :Mo <sub><i>y</i></sub> –Se core–shell nanowire array electrodes for high-performance asymmetric supercapacitors. Journal of Materials Chemistry A. 2021. 9. 27503-27517.	10.3	30
64	Benzodithiophene-thienopyrroledione-thienothiophene-based random copolymeric hole transporting material for perovskite solar cell. Chemical Engineering Journal, 2020, 382, 122830.	12.7	16
65	Hierarchical three-dimensional framework interface assembled from oxygen-doped cobalt phosphide layer-shelled metal nanowires for efficient electrocatalytic water splitting. Applied Catalysis B: Environmental, 2020, 261, 118268.	20.2	87
66	Ternary graphene-carbon nanofibers-carbon nanotubes structure for hybrid supercapacitor. Chemical Engineering Journal, 2020, 380, 122543.	12.7	157
67	Advanced Cu0.5Co0.5Se2 nanosheets and MXene electrodes for high-performance asymmetric supercapacitors. Chemical Engineering Journal, 2020, 385, 123455.	12.7	55
68	Zinc-nickel-cobalt oxide@NiMoO4 core-shell nanowire/nanosheet arrays for solid state asymmetric supercapacitors. Chemical Engineering Journal, 2020, 384, 123357.	12.7	133
69	Hexagonal boron nitride-carbon nanotube hybrid network structure for enhanced thermal, mechanical and electrical properties of polyimide nanocomposites. Composites Science and Technology, 2020, 188, 107977.	7.8	23
70	Highly reversible water splitting cell building from hierarchical 3D nickel manganese oxyphosphide nanosheets. Nano Energy, 2020, 69, 104432.	16.0	74
71	Vertically grown and intertwined Co(OH)2 nanosheet@Ni-mesh network for transparent flexible supercapacitor. Chemical Engineering Journal, 2020, 391, 123540.	12.7	44
72	Rational design of a highly mesoporous Fe–N–C/Fe <sub>3</sub> C/C–S–C nanohybrid with dense active sites for superb electrocatalysis of oxygen reduction. Journal of Materials Chemistry A, 2020, 8, 23436-23454.	10.3	33

#	Article	IF	CITATIONS
73	ZnS–Ni <sub>7</sub> S <sub>6</sub> Nanosheet Arrays Wrapped with Nanopetals of Ni(OH) <sub>2</sub> as a Novel Core–Shell Electrode Material for Asymmetric Supercapacitors with High Energy Density and Cycling Stability Performance. ACS Applied Materials & Interfaces, 2020, 12, 47377-47388.	8.0	49
74	Hierarchical CoS@MoS2 core-shell nanowire arrays as free-standing electrodes for high-performance asymmetric supercapacitors. Journal of Alloys and Compounds, 2020, 825, 154085.	5.5	19
75	High-performance solid-state hybrid supercapacitor enabled by metal–organic framework-derived multi-component hybrid electrodes of Co–N–C nanofibers and Co <sub>2â^x</sub> Fe <sub>x</sub> P–N–C micropillars. Journal of Materials Chemistry A, 2020, 8, 26158-26174.	10.3	53
76	Effects of the addition of boric acid on the physical properties of MXene/polyvinyl alcohol (PVA) nanocomposite. Composites Part B: Engineering, 2020, 199, 108205.	12.0	69
77	One-Pot Hydrothermal Synthesis of La-Doped ZnIn2S4 Microspheres with Improved Visible-Light Photocatalytic Performance. Nanomaterials, 2020, 10, 2026.	4.1	23
78	Covalent doping of Ni and P on 1T-enriched MoS <sub>2</sub> bifunctional 2D-nanostructures with active basal planes and expanded interlayers boosts electrocatalytic water splitting. Journal of Materials Chemistry A, 2020, 8, 19654-19664.	10.3	41
79	Hierarchical 3D Oxygenated Cobalt Vanadium Selenide Nanosheets as Advanced Electrode for Flexible Zinc–Cobalt and Zinc–Air Batteries. Small, 2020, 16, e2004661.	10.0	54
80	One-step electrodeposited MoS <sub>2</sub> @Ni-mesh electrode for flexible and transparent asymmetric solid-state supercapacitors. Journal of Materials Chemistry A, 2020, 8, 24040-24052.	10.3	34
81	Freestanding 1Tâ€Mn <i><sub>x</sub></i> Mo <sub>1â€"</sub> <i><sub>x</sub></i> S <sub>2â€"</sub> <i><sub>y</sub></i> and MoFe <sub>2</sub> S <sub>4â€"</sub> <i><sub>z</sub></i> Se <i><sub>z</sub></i> Ultrathin Nanosheetâ€Structured Electrodes for Highly Efficient Flexible Solidâ€State Asymmetric Supercapacitors. Small, 2020, 16, e2001691.	Se <i><sul 10.0</sul </i>	o>y <br 43
82	Molybdenum and Phosphorous Dual Doping in Cobalt Monolayer Interfacial Assembled Cobalt Nanowires for Efficient Overall Water Splitting. Advanced Functional Materials, 2020, 30, 2002533.	14.9	107
83	Highly efficient overall water splitting over a porous interconnected network by nickel cobalt oxysulfide interfacial assembled Cu@Cu <sub>2</sub> S nanowires. Journal of Materials Chemistry A, 2020, 8, 14746-14756.	10.3	34
84	Colorimetric/naked eye detection of arsenic ions in aqueous medium by mango flower extract: A facile and novel approach. Applied Surface Science, 2020, 513, 145760.	6.1	12
85	Tunable construction of FexCo3-xSe4 nanostructures as advanced electrode for boosting capacity and energy density. Chemical Engineering Journal, 2020, 390, 124557.	12.7	43
86	Rational Design of Core@shell Structured CoS <i><sub>x</sub></i> @Cu <sub>2</sub> MoS <sub>4</sub> Hybridized MoS <sub>2</sub> /N,Sâ€Codoped Graphene as Advanced Electrocatalyst for Water Splitting and Znâ€Air Battery. Advanced Energy Materials, 2020, 10, 1903289.	19.5	179
87	Flexible transparent supercapacitor with core-shell Cu@Ni@NiCoS nanofibers network electrode. Chemical Engineering Journal, 2020, 395, 125019.	12.7	82
88	Hierarchical Manganese–Nickel Sulfide Nanosheet Arrays as an Advanced Electrode for All-Solid-State Asymmetric Supercapacitors. ACS Applied Materials & Interfaces, 2020, 12, 21505-21514.	8.0	85
89	Hierarchical 3D Oxygenated Cobalt Molybdenum Selenide Nanosheets as Robust Trifunctional Catalyst for Water Splitting and Zinc–Air Batteries. Small, 2020, 16, e2000797.	10.0	52
90	All ternary metal selenide nanostructures for high energy flexible charge storage devices. Nano Energy, 2019, 65, 103999.	16.0	152

#	Article	IF	CITATIONS
91	Fabrication of Co–Ni–Zn ternary Oxide@NiWO4 core-shell nanowire arrays and Fe2O3-CNTs@GF for ultra-high-performance asymmetric supercapacitor. Composites Part B: Engineering, 2019, 176, 107223.	12.0	49
92	Metal–Organic Frameworkâ€Derived Fe/Coâ€based Bifunctional Electrode for H <sub>2</sub> Production through Water and Urea Electrolysis. ChemSusChem, 2019, 12, 4810-4823.	6.8	64
93	Effects of the composition of reduced graphene oxide/carbon nanofiber nanocomposite on charge storage behaviors. Composites Part B: Engineering, 2019, 178, 107500.	12.0	30
94	Nitrogen-doped graphene encapsulated cobalt iron sulfide as an advanced electrode for high-performance asymmetric supercapacitors. Journal of Materials Chemistry A, 2019, 7, 3941-3952.	10.3	74
95	Facile synthesis of N-doped graphene supported porous cobalt molybdenum oxynitride nanodendrites for the oxygen reduction reaction. Nanoscale, 2019, 11, 1205-1216.	5.6	27
96	g-C <sub>3</sub> N <sub>4</sub> templated synthesis of the Fe <sub>3</sub> C@NSC electrocatalyst enriched with Fe–N <sub>x</sub> active sites for efficient oxygen reduction reaction. Journal of Materials Chemistry A, 2019, 7, 16920-16936.	10.3	91
97	Bioinspired silver nanoparticles/reduced graphene oxide nanocomposites for catalytic reduction of 4-nitrophenol, organic dyes and act as energy storage electrode material. Composites Part B: Engineering, 2019, 173, 106924.	12.0	51
98	Boosting the Energy Density of Flexible Solid-State Supercapacitors via Both Ternary NiV <sub>2</sub> Se <sub>4</sub> and NiFe <sub>2</sub> Se <sub>4</sub> Nanosheet Arrays. Chemistry of Materials, 2019, 31, 4490-4504.	6.7	138
99	Hierarchical Cu@CuxO nanowires arrays-coated gold nanodots as a highly sensitive self-supported electrocatalyst for L-cysteine oxidation. Biosensors and Bioelectronics, 2019, 139, 111327.	10.1	30
100	Hydrothermal fabrication of MnCO3@rGO: A promising anode material for potassium-ion batteries. Applied Surface Science, 2019, 484, 1161-1167.	6.1	17
101	Mesoporous iron sulfide nanoparticles anchored graphene sheet as an efficient and durable catalyst for oxygen reduction reaction. Journal of Power Sources, 2019, 427, 91-100.	7.8	45
102	Hierarchically porous nickel–cobalt phosphide nanoneedle arrays loaded micro-carbon spheres as an advanced electrocatalyst for overall water splitting application. Applied Catalysis B: Environmental, 2019, 253, 235-245.	20.2	105
103	Hierarchical design of Cu-Ni(OH)2/Cu-MnxOy core/shell nanosheet arrays for ultra-high performance of asymmetric supercapacitor. Chemical Engineering Journal, 2019, 369, 705-715.	12.7	49
104	Kirkendall Growth and Ostwald Ripening Induced Hierarchical Morphology of Ni–Co LDH/MMoS <i><sub>x</sub></i> (M = Co, Ni, and Zn) Heteronanostructures as Advanced Electrode Materials for Asymmetric Solid-State Supercapacitors. ACS Applied Materials & Interfaces, 2019, 11, 11555-11567.	8.0	129
105	Metal–organic framework derived hierarchical copper cobalt sulfide nanosheet arrays for high-performance solid-state asymmetric supercapacitors. Journal of Materials Chemistry A, 2019, 7, 8620-8632.	10.3	129
106	Preparation of modified graphene oxide/polyethyleneimine film with enhanced hydrogen barrier properties by reactive layer-by-layer self-assembly. Composites Part B: Engineering, 2019, 166, 663-672.	12.0	28
107	Mesoporous layered spinel zinc manganese oxide nanocrystals stabilized nitrogen-doped graphene as an effective catalyst for oxygen reduction reaction. Journal of Colloid and Interface Science, 2019, 545, 43-53.	9.4	18
108	Constructing MoP <sub><i>x</i></sub> @MnP <sub><i>y</i></sub> Heteronanoparticle-Supported Mesoporous N,P-Codoped Graphene for Boosting Oxygen Reduction and Oxygen Evolution Reaction. Chemistry of Materials, 2019, 31, 2892-2904.	6.7	71

#	Article	IF	CITATIONS
109	A core–shell MnO <sub>2</sub> @Au nanofiber network as a high-performance flexible transparent supercapacitor electrode. Journal of Materials Chemistry A, 2019, 7, 10672-10683.	10.3	83
110	Pt nanodots monolayer modified mesoporous Cu@CuxO nanowires for improved overall water splitting reactivity. Nano Energy, 2019, 59, 216-228.	16.0	107
111	Rational design of ultrathin 2D tin nickel selenide nanosheets for high-performance flexible supercapacitors. Journal of Materials Chemistry A, 2019, 7, 24462-24476.	10.3	44
112	A spinel MnCo2O4/NG 2D/2D hybrid nanoarchitectures as advanced electrode material for high performance hybrid supercapacitors. Journal of Alloys and Compounds, 2019, 771, 810-820.	5.5	52
113	Embedded PEDOT:PSS/AgNFs network flexible transparent electrode for solid-state supercapacitor. Chemical Engineering Journal, 2019, 359, 197-207.	12.7	84
114	Electrochemical synthesis of palladium (Pd) nanorods: An efficient electrocatalyst for methanol and hydrazine electro-oxidation. Composites Part B: Engineering, 2018, 144, 11-18.	12.0	36
115	Hierarchical 3D Zn–Ni–P nanosheet arrays as an advanced electrode for high-performance all-solid-state asymmetric supercapacitors. Journal of Materials Chemistry A, 2018, 6, 8669-8681.	10.3	116
116	Hierarchical porous framework of ultrasmall PtPd alloy-integrated graphene as active and stable catalyst for ethanol oxidation. Composites Part B: Engineering, 2018, 143, 96-104.	12.0	36
117	Static and Dynamic Mechanical Properties of Graphene Oxide-Incorporated Woven Carbon Fiber/Epoxy Composite. Journal of Materials Engineering and Performance, 2018, 27, 1138-1147.	2.5	42
118	CuAg@Ag Core–Shell Nanostructure Encapsulated by N-Doped Graphene as a High-Performance Catalyst for Oxygen Reduction Reaction. ACS Applied Materials & Interfaces, 2018, 10, 4672-4681.	8.0	71
119	CdS-CoFe <sub>2</sub> O <sub>4</sub> @Reduced Graphene Oxide Nanohybrid: An Excellent Electrode Material for Supercapacitor Applications. Industrial & Engineering Chemistry Research, 2018, 57, 1350-1360.	3.7	45
120	Hierarchical material of carbon nanotubes grown on carbon nanofibers for high performance electrochemical capacitor. Chemical Engineering Journal, 2018, 345, 39-47.	12.7	66
121	Hierarchical nanohoneycomb-like CoMoO <sub>4</sub> –MnO <sub>2</sub> core–shell and Fe <sub>2</sub> O <sub>3</sub> nanosheet arrays on 3D graphene foam with excellent supercapacitive performance. Journal of Materials Chemistry A, 2018, 6, 7182-7193.	10.3	116
122	Recent advances in two-dimensional transition metal dichalcogenides-graphene heterostructured materials for electrochemical applications. Progress in Materials Science, 2018, 96, 51-85.	32.8	132
123	Enhanced gas barrier and anticorrosion performance of boric acid induced cross-linked poly(vinyl) Tj ETQq1 1 0.	784314 rg 10.3	BT /Overlock
124	Facile synthesis of 4,4′-diaminostilbene-2,2′-disulfonic-acid-grafted reduced graphene oxide and its application as a high-performance asymmetric supercapacitor. Chemical Engineering Journal, 2018, 333, 170-184.	12.7	23
125	Green synthesis of glucose-reduced graphene oxide supported Ag-Cu 2 O nanocomposites for the enhanced visible-light photocatalytic activity. Composites Part B: Engineering, 2018, 138, 35-44.	12.0	80
126	Zn-doped SnO <sub>2</sub> nano-urchin-enriched 3D carbonaceous framework for supercapacitor application. New Journal of Chemistry, 2018, 42, 955-963.	2.8	34

#	Article	IF	CITATIONS
127	Novel hydroxylated boron nitride functionalized <i>p</i> -phenylenediamine-grafted graphene: an excellent filler for enhancing the barrier properties of polyurethane. Journal of Materials Chemistry A, 2018, 6, 21501-21515.	10.3	53
128	An advanced sandwich-type architecture of MnCo <sub>2</sub> O <sub>4</sub> @N–C@MnO <sub>2</sub> as an efficient electrode material for a high-energy density hybrid asymmetric solid-state supercapacitor. Journal of Materials Chemistry A, 2018, 6, 24509-24522.	10.3	102
129	Remarkable Bifunctional Oxygen and Hydrogen Evolution Electrocatalytic Activities with Trace-Level Fe Doping in Ni- and Co-Layered Double Hydroxides for Overall Water-Splitting. ACS Applied Materials & Interfaces, 2018, 10, 42453-42468.	8.0	107
130	A New Class of Zn <sub>1</sub> <i><sub>â€x</sub></i> Fe <i><sub>x</sub></i> –Oxyselenide and Zn <sub>1â€</sub> <i><sub>x</sub></i> Fe <i><sub>x</sub></i> –LDH Nanostructured Material with Remarkable Bifunctional Oxygen and Hydrogen Evolution Electrocatalytic Activities for Overall Water Splitting. Small, 2018, 14, e1803638.	10.0	56
131	Nitrogen-Doped Graphene-Encapsulated Nickel Cobalt Nitride as a Highly Sensitive and Selective Electrode for Glucose and Hydrogen Peroxide Sensing Applications. ACS Applied Materials & Interfaces, 2018, 10, 35847-35858.	8.0	75
132	Flexible Solid‣tate Asymmetric Supercapacitors Based on Nitrogenâ€Doped Graphene Encapsulated Ternary Metalâ€Nitrides with Ultralong Cycle Life. Advanced Functional Materials, 2018, 28, 1804663.	14.9	212
133	Red, green, and blue fluorescent folate-receptor-targeting carbon dots for cervical cancer cellular and tissue imaging. Materials Science and Engineering C, 2018, 93, 1054-1063.	7.3	33
134	Hierarchical Flowerlike Highly Synergistic Three-Dimensional Iron Tungsten Oxide Nanostructure-Anchored Nitrogen-Doped Graphene as an Efficient and Durable Electrocatalyst for Oxygen Reduction Reaction. ACS Applied Materials & Interfaces, 2018, 10, 32220-32232.	8.0	48
135	Differently-charged graphene-based multilayer films by a layer-by-layer approach for oxygen gas barrier application. Composites Part B: Engineering, 2018, 155, 391-396.	12.0	29
136	Emerging core-shell nanostructured catalysts of transition metal encapsulated by two-dimensional carbon materials for electrochemical applications. Nano Today, 2018, 22, 100-131.	11.9	86
137	Highly efficient electrocatalyst of N-doped graphene-encapsulated cobalt-iron carbides towards oxygen reduction reaction. Carbon, 2018, 137, 358-367.	10.3	95
138	Highly Active and Durable Core–Shell fct-PdFe@Pd Nanoparticles Encapsulated NG as an Efficient Catalyst for Oxygen Reduction Reaction. ACS Applied Materials & Interfaces, 2018, 10, 18734-18745.	8.0	58
139	Hierarchical Heterostructures of Ultrasmall Fe <sub>2</sub> O <sub>3</sub> -Encapsulated MoS <sub>2</sub> /N-Graphene as an Effective Catalyst for Oxygen Reduction Reaction. ACS Applied Materials & Interfaces, 2018, 10, 24523-24532.	8.0	68
140	Sustainable Synthesis of Co@NC Core Shell Nanostructures from Metal Organic Frameworks via Mechanochemical Coordination Selfâ€Assembly: An Efficient Electrocatalyst for Oxygen Reduction Reaction. Small, 2018, 14, e1800441.	10.0	150
141	Fabrication of 3D graphene-CNTs/α-MoO3 hybrid film as an advance electrode material for asymmetric supercapacitor with excellent energy density and cycling life. Chemical Engineering Journal, 2018, 352, 268-276.	12.7	79
142	Graphitic carbon nitride modified graphene/Ni Al layered double hydroxide and 3D functionalized graphene for solid-state asymmetric supercapacitors. Chemical Engineering Journal, 2018, 353, 824-838.	12.7	59
143	Facile synthesis of CuCo2O4 composite octahedrons for high performance supercapacitor application. Composites Part B: Engineering, 2018, 150, 269-276.	12.0	72
144	Hierarchical NiMoS and NiFeS Nanosheets with Ultrahigh Energy Density for Flexible All Solid‣tate Supercapacitors. Advanced Functional Materials, 2018, 28, 1803287.	14.9	223

#	Article	IF	CITATIONS
145	Fabrication of a 3D Hierarchical Sandwich Co <sub>9</sub> S <sub>8</sub> /αâ€MnS@N–C@MoS <sub>2</sub> Nanowire Architectures as Advanced Electrode Material for High Performance Hybrid Supercapacitors. Small, 2018, 14, e1800291.	10.0	154
146	Enhanced physical properties of two dimensional MoS2/poly(vinyl alcohol) nanocomposites. Composites Part A: Applied Science and Manufacturing, 2018, 110, 284-293.	7.6	35
147	High-energy solid-state asymmetric supercapacitor based on nickel vanadium oxide/NG and iron vanadium oxide/NG electrodes. Applied Catalysis B: Environmental, 2018, 239, 290-299.	20.2	65
148	Cu-Au nanocrystals functionalized carbon nanotube arrays vertically grown on carbon spheres for highly sensitive detecting cancer biomarker. Biosensors and Bioelectronics, 2018, 119, 134-140.	10.1	34
149	Layer-by-layer assembled graphene oxide/polydiallydimethylammonium chloride composites for hydrogen gas barrier application. Advanced Composite Materials, 2018, 27, 457-466.	1.9	4
150	Facile synthesis of porous CuCo2O4 composite sheets and their supercapacitive performance. Composites Part B: Engineering, 2018, 150, 234-241.	12.0	51
151	Hierarchical Zn–Co–S Nanowires as Advanced Electrodes for All Solid State Asymmetric Supercapacitors. Advanced Energy Materials, 2018, 8, 1702014.	19.5	199
152	Investigation of band structure and electrochemical properties of h-BN/rGO composites for asymmetric supercapacitor applications. Materials Chemistry and Physics, 2017, 190, 153-165.	4.0	47
153	A V <sub>2</sub> O <sub>5</sub> nanorod decorated graphene/polypyrrole hybrid electrode: a potential candidate for supercapacitors. New Journal of Chemistry, 2017, 41, 1704-1713.	2.8	35
154	Polyanilineâ€Stabilized Intertwined Networkâ€like Ferrocene/Graphene Nanoarchitecture for Supercapacitor Application. Chemistry - an Asian Journal, 2017, 12, 900-909.	3.3	31
155	Layer-by-layer assembled polyelectrolyte-decorated graphene multilayer film for hydrogen gas barrier application. Composites Part B: Engineering, 2017, 114, 339-347.	12.0	40
156	Enhanced hydrogen gas barrier performance of diaminoalkane functionalized stitched graphene oxide/polyurethane composites. Composites Part B: Engineering, 2017, 117, 101-110.	12.0	40
157	Surfactant-free synthesis of NiPd nanoalloy/graphene bifunctional nanocomposite for fuel cell. Composites Part B: Engineering, 2017, 114, 319-327.	12.0	44
158	Electrochemical functionalization and in-situ deposition of the SAA@rGO/h-BN@Ni electrode for supercapacitor applications. Journal of Industrial and Engineering Chemistry, 2017, 52, 321-330.	5.8	21
159	Highly efficient adsorbent based on novel cotton flower-like porous boron nitride for organic pollutant removal. Composites Part B: Engineering, 2017, 123, 45-54.	12.0	38
160	Effects of grafting methods for functionalization of graphene oxide by dodecylamine on the physical properties of its polyurethane nanocomposites. Journal of Membrane Science, 2017, 540, 108-119.	8.2	38
161	An embedded-PVA@Ag nanofiber network for ultra-smooth, high performance transparent conducting electrodes. Journal of Materials Chemistry C, 2017, 5, 4198-4205.	5.5	35
162	Enhanced Electrochemical and Photocatalytic Performance of Core–Shell CuS@Carbon Quantum Dots@Carbon Hollow Nanospheres. ACS Applied Materials & Interfaces, 2017, 9, 2459-2468.	8.0	87

#	Article	IF	CITATIONS
163	Sunlight-driven sustainable production of hydrogen peroxide using a CdS–graphene hybrid photocatalyst. Journal of Catalysis, 2017, 345, 78-86.	6.2	130
164	A successive ionic layer adsorption and reaction (SILAR) method to fabricate a layer-by-layer (LbL) MnO 2 -reduced graphene oxide assembly for supercapacitor application. Journal of Power Sources, 2017, 340, 380-392.	7.8	51
165	A new protocol for the distribution of MnO 2 nanoparticles on rGO sheets and the resulting electrochemical performance. Applied Surface Science, 2017, 399, 95-105.	6.1	30
166	Porous Hollow‧tructured LaNiO <sub>3</sub> Stabilized N,S odoped Graphene as an Active Electrocatalyst for Oxygen Reduction Reaction. Small, 2017, 13, 1701884.	10.0	66
167	Hierarchical design of Cu <sub>1â^'x</sub> Ni <sub>x</sub> S nanosheets for high-performance asymmetric solid-state supercapacitors. Journal of Materials Chemistry A, 2017, 5, 19760-19772.	10.3	116
168	Hierarchical 3D Cobaltâ€Doped Fe <sub>3</sub> O <sub>4</sub> Nanospheres@NG Hybrid as an Advanced Anode Material for Highâ€Performance Asymmetric Supercapacitors. Small, 2017, 13, 1701275.	10.0	100
169	A hierarchical 2D Ni–Mo–S nanosheet@nitrogen doped graphene hybrid as a Pt-free cathode for high-performance dye sensitized solar cells and fuel cells. Journal of Materials Chemistry A, 2017, 5, 17896-17908.	10.3	54
170	High-energy asymmetric supercapacitors based on free-standing hierarchical Co–Mo–S nanosheets with enhanced cycling stability. Nanoscale, 2017, 9, 13747-13759.	5.6	113
171	Carbon dot stabilized copper sulphide nanoparticles decorated graphene oxide hydrogel for high performance asymmetric supercapacitor. Carbon, 2017, 122, 247-257.	10.3	130
172	Noncovalent functionalization of reduced graphene oxide with pluronic F127 and its nanocomposites with gum arabic. Composites Part B: Engineering, 2017, 128, 155-163.	12.0	50
173	A novel hierarchical 3D N-Co-CNT@NG nanocomposite electrode for non-enzymatic glucose and hydrogen peroxide sensing applications. Biosensors and Bioelectronics, 2017, 89, 970-977.	10.1	93
174	Enhanced electrocatalytic performance of an ultrafine AuPt nanoalloy framework embedded in graphene towards epinephrine sensing. Biosensors and Bioelectronics, 2017, 89, 750-757.	10.1	46
175	Facile synthesis of novel sulfonated polyaniline functionalized graphene using m-aminobenzene sulfonic acid for asymmetric supercapacitor application. Chemical Engineering Journal, 2017, 308, 1174-1184.	12.7	92
176	3D hierarchical CoO@MnO <sub>2</sub> core–shell nanohybrid for high-energy solid state asymmetric supercapacitors. Journal of Materials Chemistry A, 2017, 5, 397-408.	10.3	75
177	Fabrication of nitrogen and sulfur co-doped graphene nanoribbons with porous architecture for high-performance supercapacitors. Chemical Engineering Journal, 2017, 312, 180-190.	12.7	130
178	A novel sensitive sensor for serotonin based on high-quality of AuAg nanoalloy encapsulated graphene electrocatalyst. Biosensors and Bioelectronics, 2017, 96, 186-193.	10.1	70
179	Novel porous gold-palladium nanoalloy network-supported graphene as an advanced catalyst for non-enzymatic hydrogen peroxide sensing. Biosensors and Bioelectronics, 2016, 85, 669-678.	10.1	82
180	Facile synthesis of 3D hierarchical N-doped graphene nanosheet/cobalt encapsulated carbon nanotubes for high energy density asymmetric supercapacitors. Journal of Materials Chemistry A, 2016, 4, 9555-9565.	10.3	119

#	Article	IF	CITATIONS
181	Effective seed-assisted synthesis of gold nanoparticles anchored nitrogen-doped graphene for electrochemical detection of glucose and dopamine. Biosensors and Bioelectronics, 2016, 81, 259-267.	10.1	152
182	Facile fabrication of FeN nanoparticles/nitrogen-doped graphene core-shell hybrid and its use as a platform for NADH detection in human blood serum. Biosensors and Bioelectronics, 2016, 83, 68-76.	10.1	47
183	Peanut skin extract mediated synthesis of gold nanoparticles, silver nanoparticles and gold–silver bionanocomposites for electrochemical Sudan IV sensing. IET Nanobiotechnology, 2016, 10, 431-437.	3.8	14
184	Resveratrol cross-linked chitosan loaded with phospholipid for controlled release and antioxidant activity. International Journal of Biological Macromolecules, 2016, 93, 757-766.	7.5	36
185	Facile fabrication of highly durable Pt NPs/3D graphene hierarchical nanostructure for proton exchange membrane fuel cells. Carbon, 2016, 109, 805-812.	10.3	14
186	Effect of high molecular weight polyethyleneimine functionalized graphene oxide coated polyethylene terephthalate film on the hydrogen gas barrier properties. Composites Part B: Engineering, 2016, 106, 316-323.	12.0	40
187	Facile fabrication of Co <sub>2</sub> CuS <sub>4</sub> nanoparticle anchored N-doped graphene for high-performance asymmetric supercapacitors. Journal of Materials Chemistry A, 2016, 4, 17560-17571.	10.3	147
188	Preparation of graphene oxide/polyethyleneimine layer-by-layer assembled film for enhanced hydrogen barrier property. Composites Part B: Engineering, 2016, 92, 252-258.	12.0	31
189	Preparation and enhanced mechanical properties of non-covalently-functionalized graphene oxide/cellulose acetate nanocomposites. Composites Part B: Engineering, 2016, 90, 223-231.	12.0	71
190	In situ synthesis of graphene-encapsulated gold nanoparticle hybrid electrodes for non-enzymatic glucose sensing. Carbon, 2016, 98, 90-98.	10.3	84
191	Surface modified graphene oxide/poly(vinyl alcohol) composite for enhanced hydrogen gas barrier film. Polymer Testing, 2016, 50, 49-56.	4.8	52
192	Enhanced mechanical and thermal properties of recycled ABS/nitrile rubber/nanofil N15 nanocomposites. Composites Part B: Engineering, 2016, 93, 280-288.	12.0	36
193	Nitrogenâ€Ðoped Graphene Nanosheets with FeN Core–Shell Nanoparticles as Highâ€Performance Counter Electrode Materials for Dye‧ensitized Solar Cells. Advanced Materials Interfaces, 2016, 3, 1500348.	3.7	92
194	FeMoO4 based, enzyme-free electrochemical biosensor for ultrasensitive detection of norepinephrine. Biosensors and Bioelectronics, 2016, 81, 445-453.	10.1	41
195	Facile synthesis of vanadium nitride/nitrogen-doped graphene composite as stable high performance anode materials for supercapacitors. Journal of Power Sources, 2016, 308, 149-157.	7.8	117
196	Growth of Ni–Co binary hydroxide on a reduced graphene oxide surface by a successive ionic layer adsorption and reaction (SILAR) method for high performance asymmetric supercapacitor electrodes. Journal of Materials Chemistry A, 2016, 4, 2188-2197.	10.3	97
197	Effects of the reduction of PAni-coated oxidized multiwall carbon nanotubes on the positive temperature coefficient behaviors of their carbon black/high density polyethylene composites. Polymer Testing, 2016, 50, 83-93.	4.8	18
198	Hexylamine functionalized reduced graphene oxide/polyurethane nanocomposite-coated nylon for enhanced hydrogen gas barrier film. Journal of Membrane Science, 2016, 500, 106-114.	8.2	77

#	Article	IF	CITATIONS
199	Preparation of reduced graphene oxide-NiFe 2 O 4 nanocomposites forÂthe electrocatalytic oxidation of hydrazine. Composites Part B: Engineering, 2015, 79, 649-659.	12.0	81
200	Recent advances in graphene and its metal-oxide hybrid nanostructures for lithium-ion batteries. Nanoscale, 2015, 7, 4820-4868.	5.6	169
201	Development of high energy density supercapacitor through hydrothermal synthesis of RGO/nano-structured cobalt sulphide composites. Nanotechnology, 2015, 26, 075402.	2.6	37
202	Hydrogen gas barrier property of polyelectrolyte/ <scp>GO</scp> layerâ€byâ€layer films. Journal of Applied Polymer Science, 2015, 132, .	2.6	9
203	Novel route to synthesis of N-doped graphene/Cu–Ni oxide composite for high electrochemical performance. Carbon, 2015, 94, 962-970.	10.3	79
204	Fabrication of ultrahigh hydrogen barrier polyethyleneimine/graphene oxide films by LBL assembly fine-tuned with electric field application. Composites Part A: Applied Science and Manufacturing, 2015, 78, 60-69.	7.6	22
205	Preparation and properties of reduced graphene oxide/polyacrylonitrile nanocomposites using polyvinyl phenol. Composites Part B: Engineering, 2015, 80, 238-245.	12.0	86
206	Facile preparation of flower-like NiCo2O4/three dimensional graphene foam hybrid for high performance supercapacitor electrodes. Carbon, 2015, 89, 328-339.	10.3	132
207	Synthesis of sulfonated poly(ether ether ketone)/layered double hydroxide nanocomposite membranes for fuel cell applications. Chemical Engineering Journal, 2015, 272, 119-127.	12.7	43
208	Consequence of pH variation on the dielectric properties of Cr-doped lithium ferrite nanoparticles synthesized by the sol–gel method. Journal of Alloys and Compounds, 2015, 645, 171-177.	5.5	25
209	Electrochemical performance of reduced graphene oxide surface-modified with 9-anthracene carboxylic acid. RSC Advances, 2015, 5, 6443-6451.	3.6	34
210	N-doped carbon layer coated thermally exfoliated graphene and its capacitive behavior in redox active electrolyte. Carbon, 2015, 85, 60-71.	10.3	54
211	Epoxidation of Camelina sativa oil and peel adhesion properties. Industrial Crops and Products, 2015, 64, 1-8.	5.2	76
212	Facile synthesis of high quality multi-walled carbon nanotubes on novel 3D KIT-6: application in high performance dye-sensitized solar cells. Nanoscale, 2015, 7, 679-689.	5.6	9
213	Nicotinamide adenine dinucleotide assisted shape-controlled synthesis of catalytically active raspberry-like gold nanostructures. Electrochimica Acta, 2015, 151, 195-202.	5.2	4
214	Enhancement of physical, mechanical, and gas barrier properties in noncovalently functionalized graphene oxide/poly(vinylidene fluoride) composites. Carbon, 2015, 81, 329-338.	10.3	84
215	Polymer-Layered Silicate Nanocomposite Membranes for Fuel Cell Application. , 2014, , 481-509.		1
216	Effects of ionic liquid-functionalized mesoporous silica on the proton conductivity of acid-doped poly(2,5-benzimidazole) composite membranes for high-temperature fuel cells. Journal of Membrane Science, 2014, 449, 136-145.	8.2	55

#	Article	IF	CITATIONS
217	Enhanced properties of aryl diazonium salt-functionalized graphene/poly(vinyl alcohol) composites. Chemical Engineering Journal, 2014, 245, 311-322.	12.7	42
218	Preparation and characterization of self-assembled layer by layer NiCo2O4–reduced graphene oxide nanocomposite with improved electrocatalytic properties. Journal of Alloys and Compounds, 2014, 590, 266-276.	5.5	109
219	lodide-mediated room temperature reduction of graphene oxide: a rapid chemical route for the synthesis of a bifunctional electrocatalyst. Journal of Materials Chemistry A, 2014, 2, 1332-1340.	10.3	137
220	Synthesis, magnetic and Mössbauer spectroscopic studies of Cr doped lithium ferrite nanoparticles. Journal of Alloys and Compounds, 2014, 591, 174-180.	5.5	42
221	Hydrothermal synthesis of Fe <sub>3</sub> O <sub>4</sub> /RGO composites and investigation of electrochemical performances for energy storage applications. RSC Advances, 2014, 4, 44777-44785.	3.6	54
222	Enhanced mechanical properties of a multiwall carbon nanotube attached pre-stitched graphene oxide filled linear low density polyethylene composite. Journal of Materials Chemistry A, 2014, 2, 2681-2689.	10.3	42
223	Effects of surface-modified silica nanoparticles attached graphene oxide using isocyanate-terminated flexible polymer chains on the mechanical properties of epoxy composites. Journal of Materials Chemistry A, 2014, 2, 10557-10567.	10.3	78
224	Layer-structured graphene oxide/polyvinyl alcohol nanocomposites: dramatic enhancement of hydrogen gas barrier properties. Journal of Materials Chemistry A, 2014, 2, 12158.	10.3	71
225	Reduced graphene oxide (RGO)-supported NiCo <sub>2</sub> O <sub>4</sub> nanoparticles: an electrocatalyst for methanol oxidation. Nanoscale, 2014, 6, 10657.	5.6	177
226	7,7,8,8-Tetracyanoquinodimethane-assisted one-step electrochemical exfoliation of graphite and its performance as an electrode material. Nanoscale, 2014, 6, 4864-4873.	5.6	52
227	Simultaneous reduction, exfoliation, and nitrogen doping of graphene oxide via a hydrothermal reaction for energy storage electrode materials. Carbon, 2014, 69, 66-78.	10.3	169
228	Enhanced mechanical properties and proton conductivity of Nafion–SPEEK–GO composite membranes for fuel cell applications. Journal of Membrane Science, 2014, 458, 128-135.	8.2	80
229	Effects of acid vapour mediated oxidization on the electrochemical performance of thermally exfoliated graphene. Carbon, 2014, 74, 195-206.	10.3	24
230	Characterizations of in situ grown ceria nanoparticles on reduced graphene oxide as a catalyst for the electrooxidation of hydrazine. Journal of Materials Chemistry A, 2013, 1, 9792.	10.3	234
231	Enhanced mechanical properties of silanized silica nanoparticle attached graphene oxide/epoxy composites. Composites Science and Technology, 2013, 79, 115-125.	7.8	331
232	Effects of covalent surface modifications on the electrical and electrochemical properties of graphene using sodium 4-aminoazobenzene- $4\hat{a}\in^2$ -sulfonate. Carbon, 2013, 54, 310-322.	10.3	65
233	Synthesis and characterization of novel thiophene-based polybenzimidazole membrane for high-temperature fuel cells. Journal of Applied Electrochemistry, 2013, 43, 749-754.	2.9	3
234	Efficient reduction of graphene oxide using Tin-powder and its electrochemical performances for use as an energy storage electrode material. Journal of Materials Chemistry A, 2013, 1, 11320.	10.3	15

#	Article	IF	CITATIONS
235	UV-curable pressure-sensitive adhesives derived from functionalized soybean oils and rosin ester. Polymer International, 2013, 62, 1293-1301.	3.1	37
236	Controlled, Defect-Guided, Metal-Nanoparticle Incorporation onto MoS <sub>2</sub> via Chemical and Microwave Routes: Electrical, Thermal, and Structural Properties. Nano Letters, 2013, 13, 4434-4441.	9.1	281
237	Effects of reduction and polystyrene sulfate functionalization on the capacitive behaviour of thermally exfoliated graphene. Journal of Materials Chemistry A, 2013, 1, 5892.	10.3	33
238	Effects of dual component microcapsules of resin and curing agent on the self-healing efficiency of epoxy. Composites Part B: Engineering, 2013, 55, 79-85.	12.0	124
239	Effects of processing conditions of poly(methylmethacrylate) encapsulated liquid curing agent on the properties of self-healing composites. Composites Part B: Engineering, 2013, 49, 6-15.	12.0	122
240	UV-Curable, High-Shear Pressure-Sensitive Adhesives Derived from Acrylated Epoxidized Soybean Oil. Journal of Adhesion, 2013, 89, 323-338.	3.0	15
241	Preparation of sulfonated poly(ether–ether–ketone) functionalized ternary graphene/AuNPs/chitosan nanocomposite for efficient glucose biosensor. Process Biochemistry, 2013, 48, 1724-1735.	3.7	54
242	One-step electrochemical synthesis of 6-amino-4-hydroxy-2-napthalene-sulfonic acid functionalized graphene for green energy storage electrode materials. Nanotechnology, 2013, 24, 365706.	2.6	34
243	Effects of sodium hydroxide on the yield and electrochemical performance of sulfonated poly(ether-ether-ketone) functionalized graphene. Journal of Materials Chemistry A, 2013, 1, 9294.	10.3	34
244	In situ synthesis of the reduced graphene oxide–polyethyleneimine composite and its gas barrier properties. Journal of Materials Chemistry A, 2013, 1, 3739.	10.3	236
245	Recent advances in the efficient reduction of graphene oxide and its application as energy storage electrode materials. Nanoscale, 2013, 5, 52-71.	5.6	432
246	Simultaneous reduction, functionalization and stitching of graphene oxide with ethylenediamine for composites application. Journal of Materials Chemistry A, 2013, 1, 1349-1358.	10.3	204
247	Effects of hybrid carbon fillers of polymer composite bipolar plates on the performance of direct methanol fuel cells. Composites Part B: Engineering, 2013, 51, 98-105.	12.0	39
248	Electrostatically assembled layer-by-layer composites containing graphene oxide for enhanced hydrogen gas barrier application. Composites Science and Technology, 2013, 89, 167-174.	7.8	55
249	Effects of various surfactants on the dispersion stability and electrical conductivity of surface modified graphene. Journal of Alloys and Compounds, 2013, 562, 134-142.	5.5	91
250	Synergistic effects of oxidized CNTs and reactive oligomer on the fracture toughness and mechanical properties of epoxy. Composites Part A: Applied Science and Manufacturing, 2013, 49, 58-67.	7.6	33
251	Micro-crack behavior of carbon fiber reinforced thermoplastic modified epoxy composites for cryogenic applications. Composites Part B: Engineering, 2013, 44, 533-539.	12.0	84
252	Tin-Powder Mediated Facile Route for the Reduction of Graphene Oxide. Advanced Materials Research, 2013, 747, 238-241.	0.3	0

#	Article	IF	CITATIONS
253	Electrochemically exfoliated graphene using 9-anthracene carboxylic acid for supercapacitor application. Journal of Materials Chemistry, 2012, 22, 24403.	6.7	87
254	Protic ionic liquid-functionalized mesoporous silica-based hybrid membranes for proton exchange membrane fuel cells. Journal of Materials Chemistry, 2012, 22, 24366.	6.7	51
255	Dual role of glycine as a chemical functionalizer and a reducing agent in the preparation of graphene: an environmentally friendly method. Journal of Materials Chemistry, 2012, 22, 9696.	6.7	222
256	Facile Method for the Preparation of Water Dispersible Graphene using Sulfonated Poly(ether–ether–ketone) and Its Application as Energy Storage Materials. Langmuir, 2012, 28, 9825-9833.	3.5	85
257	Carbon-based nanostructured materials and their composites as supercapacitor electrodes. Journal of Materials Chemistry, 2012, 22, 767-784.	6.7	672
258	Synthesis and Characterization of Amphiphilic Reduced Graphene Oxide with Epoxidized Methyl Oleate. Advanced Materials, 2012, 24, 2123-2129.	21.0	25
259	A green approach for the reduction of graphene oxide by wild carrot root. Carbon, 2012, 50, 914-921.	10.3	337
260	Simultaneous bio-functionalization and reduction of graphene oxide by baker's yeast. Chemical Engineering Journal, 2012, 183, 526-533.	12.7	250
261	Tunable electrical conductivity and dielectric properties of triglycine sulfate-polypyrrole composite. Chemical Engineering Journal, 2012, 187, 334-340.	12.7	18
262	Effect of peptizer on the properties of Nafion–Laponite clay nanocomposite membranes for polymer electrolyte membrane fuel cells. Journal of Membrane Science, 2012, 389, 316-323.	8.2	28
263	Poly(2,5-benzimidazole)–silica nanocomposite membranes for high temperature proton exchange membrane fuel cell. Journal of Membrane Science, 2012, 411-412, 91-98.	8.2	47
264	Chemical functionalization of graphene and its applications. Progress in Materials Science, 2012, 57, 1061-1105.	32.8	1,612
265	Effect of functionalized graphene on the physical properties of linear low density polyethylene nanocomposites. Polymer Testing, 2012, 31, 31-38.	4.8	184
266	Functionalized-graphene/ethylene vinyl acetate co-polymer composites for improved mechanical and thermal properties. Polymer Testing, 2012, 31, 282-289.	4.8	114
267	Material selection windows for hybrid carbons/poly(phenylene sulfide) composite for bipolar plates of fuel cell. Polymer Testing, 2012, 31, 537-545.	4.8	37
268	Silicate-based polymer-nanocomposite membranes for polymer electrolyte membrane fuel cells. Progress in Polymer Science, 2012, 37, 842-869.	24.7	186
269	Effect of reactive poly(ethylene glycol) flexible chains on curing kinetics and impact properties of bisphenolâ€a glycidyl ether epoxy. Journal of Applied Polymer Science, 2012, 124, 2325-2332.	2.6	8
270	Preparation of non-covalently functionalized graphene using 9-anthracene carboxylic acid. Nanotechnology, 2011, 22, 405603.	2.6	48

Nam Hoon Kim

#	Article	IF	CITATIONS
271	Preparation of water-dispersible graphene by facile surface modification of graphite oxide. Nanotechnology, 2011, 22, 305710.	2.6	91
272	Electrochemical performance of a graphene–polypyrrole nanocomposite as a supercapacitor electrode. Nanotechnology, 2011, 22, 295202.	2.6	146
273	Characterization and properties of in situ emulsion polymerized poly(methyl methacrylate)/graphene nanocomposites. Composites Part A: Applied Science and Manufacturing, 2011, 42, 1856-1861.	7.6	156
274	Surface Reaction of LiCoO <sub>2</sub> /Li System under High-Voltage Conditions by X-Ray Spectroscopy and Two-Dimensional Correlation Spectroscopy (2D-COS). Applied Spectroscopy, 2011, 65, 320-325.	2.2	12
275	Aniline- and N,N-dimethylformamide-assisted processing route for graphite nanoplates: intercalation and exfoliation pathway. Materials Letters, 2011, 65, 1371-1374.	2.6	5
276	Recent advances in graphene-based biosensors. Biosensors and Bioelectronics, 2011, 26, 4637-4648.	10.1	1,184
277	Lipaseâ€catalyzed synthesis and characterization of biodegradable polyester containing <scp>l</scp> â€malic acid unit in solvent system. Journal of Applied Polymer Science, 2011, 120, 1114-1120.	2.6	31
278	New hyperbranched polymers for membranes of highâ€ŧemperature polymer electrolyte membrane fuel cells: Determination of the crystal structure and freeâ€volume size. Journal of Applied Polymer Science, 2011, 121, 923-929.	2.6	12
279	Efficient synthesis of graphene sheets using pyrrole as a reducing agent. Carbon, 2011, 49, 3497-3502.	10.3	201
280	Preparation of functionalized graphene/linear low density polyethylene composites by a solution mixing method. Carbon, 2011, 49, 1033-1037.	10.3	336
281	Polymer membranes for high temperature proton exchange membrane fuel cell: Recent advances and challenges. Progress in Polymer Science, 2011, 36, 813-843.	24.7	796
282	Effects of the surface treatment on the properties of polyaniline coated carbon nanotubes/epoxy composites. Composites Part B: Engineering, 2010, 41, 2-7.	12.0	38
283	Synergy effects of hybrid carbon system on properties of composite bipolar plates for fuel cells. Journal of Power Sources, 2010, 195, 5474-5480.	7.8	37
284	Effect of surface treatment with potassium persulfate on dispersion stability of multi-walled carbon nanotubes. Materials Letters, 2010, 64, 718-721.	2.6	11
285	Synergy effect of hybrid fillers on the positive temperature coefficient behavior of polypropylene/ultraâ€high molecular weight polyethylene composites. Journal of Applied Polymer Science, 2010, 116, 116-124.	2.6	63
286	Synthesis of water soluble sulfonated polyaniline and determination of crystal structure. Journal of Applied Polymer Science, 2010, 117, 2025-2035.	2.6	37
287	Recent advances in graphene based polymer composites. Progress in Polymer Science, 2010, 35, 1350-1375.	24.7	2,949
288	A new self-cross-linked, net-structured, proton conducting polymer membrane for high temperature proton exchange membrane fuel cells. Journal of Membrane Science, 2010, 349, 304-311.	8.2	67

#	Article	IF	CITATIONS
289	Hyperbranched poly(benzimidazole-co-benzene) with honeycomb structure as a membrane for high-temperature proton-exchange membrane fuel cells. Journal of Power Sources, 2010, 195, 2470-2477.	7.8	39
290	In-situ synthesis and characterization of electrically conductive polypyrrole/graphene nanocomposites. Polymer, 2010, 51, 5921-5928.	3.8	464
291	Heating fluid from aqueous dispersion of metallic to semiconducting particles. International Journal of Thermal Sciences, 2010, 49, 2000-2007.	4.9	2
292	Surface characterization of the high voltage LiCoO2/Li cell by X-ray photoelectron spectroscopy and 2D correlation analysis. Vibrational Spectroscopy, 2010, 53, 60-63.	2.2	17
293	Effects of surface modification on the dispersion and electrical conductivity of carbon nanotube/polyaniline composites. Scripta Materialia, 2009, 60, 551-554.	5.2	108
294	Poly(acrylamide/laponite) nanocomposite hydrogels: Swelling and cationic dye adsorption properties. Journal of Applied Polymer Science, 2009, 111, 1786-1798.	2.6	50
295	Swelling behavior of polyacrylamide/laponite clay nanocomposite hydrogels: pH-sensitive property. Composites Part B: Engineering, 2009, 40, 275-283.	12.0	71
296	Effect of carbon fillers on properties of polymer composite bipolar plates of fuel cells. Journal of Power Sources, 2009, 193, 523-529.	7.8	138
297	Investigation of multiâ€walled carbon nanotubeâ€reinforced highâ€density polyethylene/carbon black nanocomposites using electrical, DSC and positron lifetime spectroscopy techniques. Polymer International, 2009, 58, 775-780.	3.1	47
298	Preparation of nanosize polyaniline by solidâ€state polymerization and determination of crystal structure. Polymer International, 2009, 58, 1173-1180.	3.1	50
299	Positive temperature coefficient characteristic and structure of graphite nanofibers reinforced high density polyethylene/carbon black nanocomposites. Composites Part B: Engineering, 2009, 40, 218-224.	12.0	81
300	Improved mechanical and swelling behavior of the composite hydrogels prepared by ionic monomer and acid-activated Laponite. Applied Clay Science, 2009, 46, 414-417.	5.2	59
301	Synthesis and characterization of polyanilineâ€multiwalled carbon nanotube nanocomposites in the presence of sodium dodecyl sulfate. Polymers for Advanced Technologies, 2008, 19, 1754-1762.	3.2	89
302	Novel PAAm/Laponite clay nanocomposite hydrogels with improved cationic dye adsorption behavior. Composites Part B: Engineering, 2008, 39, 756-763.	12.0	87
303	Miscibility and compatibilization of poly(trimethylene terephthalate)/acrylonitrile–butadiene–styrene blends. European Polymer Journal, 2007, 43, 3826-3837.	5.4	49
304	Effects of the addition of multi-walled carbon nanotubes on the positive temperature coefficient characteristics of carbon-black-filled high-density polyethylene nanocomposites. Scripta Materialia, 2006, 55, 1119-1122.	5.2	130
305	Nafion-Peptized Laponite Clay Nanocomposite Membrane for PEMFC. Advanced Materials Research, 0, 410, 148-151.	0.3	1
306	A Facile One-Step Hydrothermal Synthesis of Graphene/CeO <sub>2</sub> Nanocomposite and its Catalytic Properties. Advanced Materials Research, 0, 747, 242-245.	0.3	12

#	Article	IF	CITATIONS
307	Electrochemically Preparation of Functionalized Graphene Using Sodium Dodecyl Benzene Sulfonate (SDBS). Advanced Materials Research, 0, 747, 246-249.	0.3	11
308	Synthesis and Characterization of SPEEK/Layered Double Hydroxide Polymer Nanocomposite for Fuel Cell Applications. Advanced Materials Research, 0, 747, 234-237.	0.3	9